Experimental investigation of granular dynamics close to the jamming transition

2005 J. Phys.: Condens. Matter 17 S2503

(http://iopscience.iop.org/0953-8984/17/24/009)

INSTITUTE OF PHYSICS PUBLISHING JOURNAL OF PHYSICS: CONDENSED MATTER

J. Phys.: Condens. Matter **17** (2005) S2503–S2516 doi:10.1088/0953-8984/17/24/009

Experimental investigation of granular dynamics close to the jamming transition

G Caballero, E Kolb, A Lindner, J Lanuza and E Clément

Laboratoire de Physique et Mécanique des Milieux Hétérogènes, ESPCI, 10 rue Vauquelin, 75231 Paris Cedex 05, France

Received 4 April 2005
Published 3 June 2005
Online at stacks.iop.org/JPhysCM/17/S2503

Abstract

We present different experiments on dense granular assemblies with the aim of clarifying the notion of 'jamming transition' for these assemblies of non-Brownian particles. The experimental set-ups differ in the way in which external perturbations are applied in order to unjam the systems. The first experiment monitors the response to a locally applied deformation of a model packing at rest. The two other experiments study local and collective dynamics in a granular assembly weakly excited by vibration.

1. Introduction

The dynamical behaviour of a granular medium in the dense regime is very intriguing [1, 2]. Much of the interest lies in the analogies that can be found with glass forming liquids characterized by a diverging viscosity and an arrest of the flow at the approach to the glass transition [3]. Although the grains are non-Brownian particles, granular media are also characterized by a slower and more complex dynamics when the packing fraction of the assembly and/or the confining pressure increases. Then, the granular packing enters into an apparently jammed state characterized by the onset of a yield stress and of ageing properties as is observed in many other amorphous systems [4]. This led Liu and Nagel [5] to propose a phase diagram unifying the concept of jamming in systems as different as emulsions, foams, granular systems, colloidal suspensions and glasses. In all these amorphous systems, the system unjams and the flow is initiated by applying a sufficiently high external shear stress, lowering the packing fraction or increasing the temperature. By analogy with the behaviour of supercooled liquids the authors speculated that there might be an equivalent of a temperature in athermal systems like for granular media and that a thermodynamics based on this effective temperature could be relevant. However there are different ways of defining a temperature and the question is not yet solved [6–9]. Here we are dealing with assemblies of grains with a size larger than a micrometre. In this condition, no coupling with thermodynamic temperature via Brownian motion exists. Due to the dissipative interaction between the grains, a granular

assembly without energy input is at rest in a metastable state, at a 'zero temperature' in the kinetic sense. To activate motion and 'unjam' the packing one has to supply energy which can be done in various ways (shearing, avalanching, vibrating, external fluid pressure, ...).

In this paper we propose three new experimental ways to study the dynamics of a granular packing in the vicinity of a jammed state. The first deals with a model 2D jammed assembly in which motion of the grains is obtained by a local application of a displacement sufficient to create motion of the grains. We are interested in the range of mobilization of the grains and in the reversible aspect of the motion. The second and the third experiments are concerned with granular assemblies excited by vibration. We design two new ways of injecting energy into a granular packing that will be suitable for studying in detail the dynamical properties in the vicinity of the jammed state and help in investigating the notion of effective temperature.

2. Local unjamming of a 'zero-temperature' granular assembly

The principle of this 2D model experiment is simple: it consists in perturbing weakly and locally a dense granular packing by displacing one of the grains (the intruder) with a given small amplitude. Quasi-static perturbation cycles are performed to monitor the packing evolution through the mean displacement field around the intruder. The experiment, using hard grains, is a sensitive mechanical test of the structural stability exhibited by dense granular assemblies far above the elastic limit and also far below the usual fully developed plasticity domain. From a practical point of view it bears similarities with standard penetrometry tests currently used in soil mechanics. A more precise account of this experiment can be found in Kolb *et al* [10]. We find that the displacement fields in response to the local perturbation are quite long range in the direction of the perturbation and evolving quite a bit. In a finite but large number of cycles, a quasi-reversible response is achieved. However in this limit we also evidence a remanent irreversibility field spanning the whole system. We also propose here new results on the effect of a slight difference in the preparation procedure. The fact that no thermal activation is present means that after the preparation stage, many configurations, more or less unstable and characteristic of the preparation, are 'frozen' in the dense phase and that the initial mechanical response may be strongly sensitive to the packing history. We compare the evolution of the response function through the cycling procedure and we show that the initial configurations prepared by quasi-static agitation at constant volume or under a weak tapping have clearly different responses even though the mean packing fractions obtained in these two cases are extremely close.

2.1. Experimental set-up

The grains are metallic cylinders of outer diameters $d_1 = 4$ mm and $d_2 = 5$ mm. The proportion of grains of each size is chosen in order to form a disordered packing. Here, the grains are rigid and such that the detected displacements are due to granular rearrangements, i.e. changing the contact positions and status (opening and closing), and not due to the deformation of contacts between the grains. About 4000 grains are piled up onto an initially horizontal glass plate surrounded by plexiglass walls forming a rectangular box of width $L = 26.8$ cm ($\sim 54 d_2$) (figure 1, left part). For the first preparation method that we describe initially, the configuration of grains is changed at a fixed volume by applying manually sequences of quasi-random perturbations. Then, the plate is slowly tilted up to an angle $\varphi = 33°$, corresponding to a value above the typical angle of friction of the grains on the glass plate (25°). The overall height of grains is $H = 34.4$ cm ($\sim 70 d_2$) and the packing is left with an open free surface for the experiment. The 2D packing fraction is then $\phi = 0.749 \pm 0.004$.

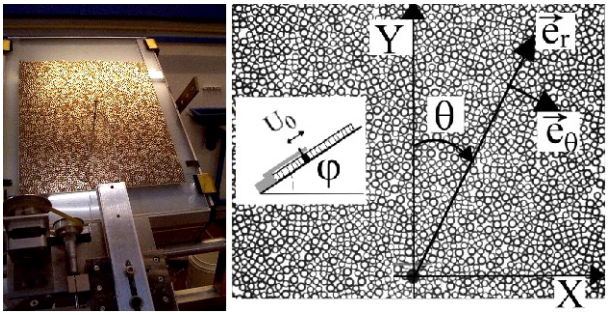

Figure 1. Left: photo of the experimental set-up. Right: typical frame of observation of the piling. The intruder is below the black point (inset: sketch of the experimental set-up viewed from the side)

The so-called 'intruder' grain that will be displaced is located in the bulk at a depth of $h \cong 2/3\ H \cong 40d_2$ from the free surface. The perturbation consists in a controlled and cyclic displacement along the direction of effective gravity (the Y axis; see figure 1, right part). The motion of the intruder is quasi-static and small with an amplitude of $U_0 = 1.25$ mm ($\sim d_2/3$) giving a typical strain less than 10^{-2}. Note that the induced strain is large compared to the estimated perturbation in the case of the typical force response function tested for example in Reydellet *et al* [11] but small compared to fully developed plasticity [12]. Unlike these experiments, ours has no information on forces but it does have information on displacements of grains. The elastic deformations at the contacts are much smaller than what we can detect for our rigid discs.

2.2. *Displacement response functions*

At each stage of perturbation, the reorganizations can be precisely followed by taking pictures before and after a given perturbation by use of a high resolution CCD camera (1280×1024 pixels^2). A subsequent fine subpixel analysis is used by correlating the image on grey levels with referenced images corresponding to both kinds of cylinders. This analysis allows one to detect the centres of particles with a high resolution of 0.05 pixels ($\sim d_2/600$). Then the displacements of each grain are calculated in response to the upward motions and downward motions of the intruder (the corresponding displacements are denoted respectively as $\vec{u}_\uparrow$ and $\vec{u}_\downarrow$). The first motion ($i = 1$) of the intruder is always upwards so that the ith displacement field corresponding to an upward (respectively downward) motion of the intruder is associated with an odd (resp. even) value of i.

Now we focus on the displacement response due to the upward motions of the intruder. We observe that even a perturbation as small as $U_0 \simeq d_2/3$ induces noticeable displacements far above the intruder. It is still possible to observe displacements up to the limit of our frame corresponding to a distance of 30 grains above the intruder. In order to extract quantitative information, we used a binning of 40 pixels ($1.2d_2$) to divide the frame into square cells and averaged the responses for a given cycle n in each cell over 16 experiments prepared in identical conditions. The contact networks (and certainly also the force networks) differ from one realization to another and the displacement responses differ significantly. However here we want to obtain information on an ensemble of realizations with a given preparation and packing fraction. From our image processing and binning method we thus extract a mean displacement field by averaging over several realizations for a given preparation and packing fraction. Then

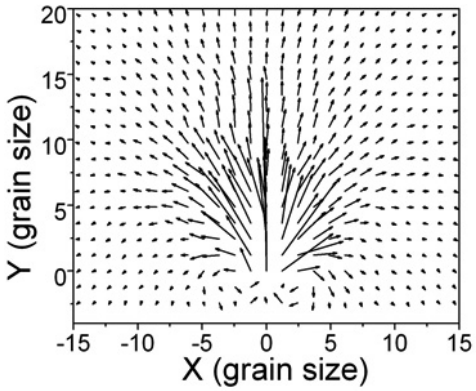

Figure 2. Mean displacement field $\overrightarrow{u}_n^{\uparrow}$ for the second upward motion of the intruder ($i = 3$ or $n = 2$). All displacements have been magnified by a factor of 70. The intruder is located at $X = 0, Y = 0$.

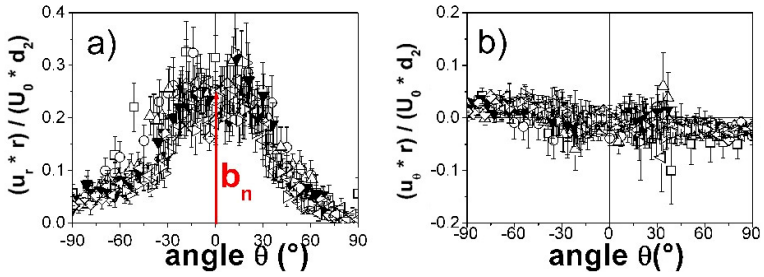

Figure 3. Rescaled and adimensionalized components of the mean response functions in polar coordinates for the ninth upward motion of the intruder ($i = 17$ or $n = 9$). Radial $\lambda_{n,r}(r, \theta)$ (a) and azimuthal $\mu_{n,r}(r, \theta)$ (b) components are plotted against the angle θ from the vertical. The data collapses observed for (a) and (b) have been obtained with radial distances r ranging from $7.4d_2$ to $21.8d_2$, represented by different symbols, e.g. the downward-pointing solid triangle for $r = 15.8d_2$. The quantity b_n is the maximum of the mean profile (a).

the mean upward displacement field $u_n^{\uparrow}$ (figure 2) obtained for the first preparation clearly evidences the long range of the perturbation with a quasi-radial displacement field above the intruder. We also observe the presence of two antisymmetrical rolls on each side of the intruder which are reversed when the perturbation changes its direction. The typical decay of the response with the radial distance r from the intruder is analysed. After several cycles the response to an upward perturbation exhibits a $1/r^{\alpha}$ dependence where α is close to 1. This is shown by renormalizing the radial $u_{n,r}$ and azimuthal $u_{n,\theta}$ components of the displacement field $\overrightarrow{u}_n^{\uparrow} = u_{n,r}\overrightarrow{e_r} + u_{n,\theta}\overrightarrow{e_\theta}$ by r and plotting the adimensional and renormalized components $\lambda_{n,r}(r, \theta) = r \cdot u_{n,r}/(U_0 d_2)$ and $\mu_{n,r}(r, \theta) = r \cdot u_{n,\theta}/(U_0 d_2)$ (see figure 1 for the notation). In the limit of the experimental uncertainties the azimuthal response $\mu_{n,r}(r, \theta)$ (figure 3(b)) is almost zero while the radial responses $\lambda_{n,r}(r, \theta)$ (figure 3(a)) superimpose for different values r with a typical bell shape curve $f(\theta)$. The response can therefore be modelled by the following relation:

$$\overrightarrow{u}_n^{\uparrow} \simeq b_n U_0 d_2 \frac{f(\theta)}{r} \overrightarrow{e}_r, \tag{1}$$

which is valid in the upper part above the intruder for a distance larger than $7d_2$.

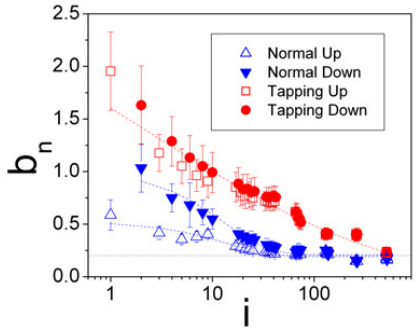

Figure 4. Evolution of the typical amplitude of the response b_n (defined in the preceding figure) as a function of the number i of displacements of the intruder with $n = \text{int}(\frac{i+1}{2})$. The triangles correspond to the response for a normal preparation, with the upward-pointing (resp. downward-pointing) symbols for the response to an upward (resp. downward) perturbation. The square and points are defined in the same way for preparation by tapping. The dashed lines are guides for the eye.

2.3. Response function evolution: reversibility/irreversibility

To follow the response evolution through the cycles we monitor the dimensionless parameter b_n characterizing the renormalized amplitude of the response in the upper vertical direction: $\lambda_r(r, \theta = 0)$, averaged over distances larger than $7d_2$. The error bar witnesses rms statistical deviations from the average. This parameter b_n decreases with n as shown in figure 4 and seems to saturate at a constant level with $b_n = 0.19 \pm 0.01$ after about $n \sim 30$ cycles (or $i \sim 60$ displacements of the intruder). For the downward responses we also measure the corresponding b_n but we must note that in this case, we do not have rigorously a $1/r$ decay but rather a $1/r^{\gamma}$ decay with γ evolving from 0.5 to 1 as n increases. Actually, in this case, the large error bars take this effect into account. Because effective gravity acts in the same direction as the perturbation for downward motion of the intruder, the mean response is larger in this case (see the differences between upward-pointing and downward-pointing triangles in figure 4). The difference between up and down mean responses leads to a small irreversibilty at each cycle. Note that in spite of these irreversible displacements, the packing fraction stays constant within $5/1000$. But after $n \sim 30$ cycles, the mean responses for upward and downward motions of the intruder are almost identical: a quasi-stationary regime or 'limit cycle' is obtained.

Once the mean irreversible field disappears and the quasi-stationary regime is reached, we can still witness an irreversible component of the displacement field but of very small amplitude. It is vizualized on figure 5 by plotting the cumulative displacements of grains between the images $i = 129$ and $i + 2p = 513$ both taken in the low position of the intruder, in the regime where the mean response does not evolve. It is interesting to note the existence of large heterogeneities of displacements (and therefore of mobilities) and the presence of long range streams besides vortex-like structures. These structures depend on the configurations of the packing and disappear when averaged over many realizations. A detailed analysis of these structures would be interesting in comparison with what is observed in glass forming liquids at the approach of the glass temperature.

2.4. Dependence on preparation

Another important feature is the dependence of the range of the perturbation on small changes of the initial preparation. We now compare two modes of preparation: the original one obtained

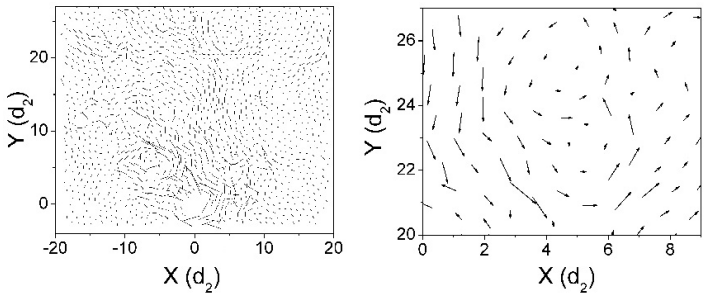

Figure 5. Irreversible displacement field for a given realization. The arrows represent the cumulative displacement of each grain between the images $i = 129$ and 513 (magnified by a factor of 20). The figure on the right is a zoom of a vortex-like field obtained in the dotted subframe of the figure on the left.

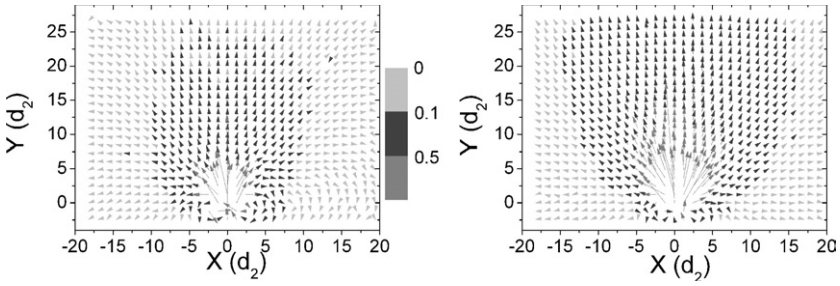

Figure 6. Mean upward displacement field for normal (left) and tapping (right) preparations for the ninth cycle. The greyscale code corresponds to different amplitudes of displacements given in pixels. Recall that 33 pixels corresponds to the diameter of a big grain d_2.

by random initial restructuring at constant volume and the so-called 'tapping one' consisting in tapping the walls of the inclined container just before beginning the experiment. Note that a very similar initial packing fraction is obtained by this second preparation; then $\phi = 0.750 \pm 0.002$. However the effects on the subsequent response observed via the displacement field are quite visible as can be observed in figure 6 with greyscale codes corresponding to different amplitudes of displacements. We clearly observe that the response for tapping preparation is enhanced and more directive in the direction of gravity. The mean displacement field on the axis of the perturbation still decays as a power law with the distance from the intruder but the exponent of this $1/r^{\alpha}$ decay is closer to $\alpha \approxeq 0.5$, quite similar to the one observed for downward motion of the intruder. This exponent evolves with the number of cycles and finally reaches $\alpha \approxeq 1$.

Although there is no linear rescaling with r, the parameter b_n is still used for comparing the response with the normal preparation one. The square and point curves of figure 4 show that the response is larger for tapping preparation. We also observe a decrease of the response with n but no clear saturation of the response even if the mean irreversibility also tends to zero after about the same number of cycles as before, i.e. $n \sim 30$ cycles. In both cases, changes in packing fraction during the experiment are less than $5/1000$ and certainly would not explain such differences in the evolution process. It is then natural to look for the influence of local configuration parameters such as the evolution of the contact angle distribution or other texture parameters. Until now the only significant differences we could note between the outcomes of these two preparation routes are in the initial mean coordination number which is a finer parameter than the packing fraction. The tapping preparation gives an initial higher

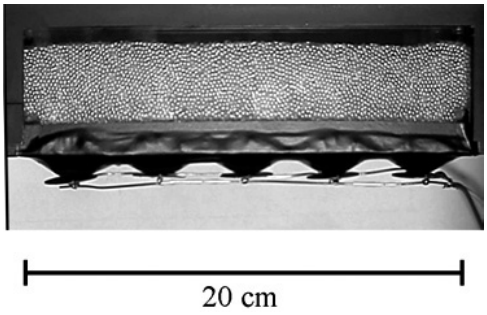

Figure 7. Experimental set-up: five piezoelectric transducers form the bottom of a rectangular glass box which is filled with 1.5 mm glass beads. The piezos are excited by a 400 Hz square signal with a maximum effective voltage $V_{\text{eff}} = 9$ V.

coordination number with a relative increase of 2% compared with the normal preparation one, thus leading to a more 'jammed' system.

3. Internal dynamics of a weakly thermalized granular packing

3.1. Thermalization by sound injection of a 3D granular assembly

To unjam a granular material, it is possible to provide energy to the system by shaking. It was shown that for vibration accelerations larger than the acceleration of gravity one can reach dynamical states close to those of liquids and gases. For moderate agitation one obtains very condensed states with reduced mobility which are phenomenologically akin to glassy phases. In this regime an interesting compaction dynamics was observed associated with slow relaxation and memory effects [13–18]. So far, vibration was applied by tapping a container filled with grains, with the disadvantage of maximizing boundary effects and involving complicated grain–container interaction phenomena like convection. Moreover, reaching precisely a glassy limit is quite difficult since one has to tune the tap acceleration close to the gravity level very precisely, and this in a regime where boundary friction is dominant. Furthermore, the energy transfer is quite complex since the packing is periodically accelerated with a mixture of 'free' falls of the packing and up-going shock waves.

Here, we present an experimental set-up that allows one to vibrate a granular material in a novel way. In our set-up the grains are in direct contact with five piezoelectric transducers (see figure 7) which create a quasi-randomly agitated surface in connection with the bulk of the packing—a kind of 'thermal' bath. Each transducer is at the bottom of a conical shaped paper container and all of them constitute the bottom of a hollow rectangular box of 20 cm in length, 2.3 cm in width and around 4 cm in height. The front and rear boundaries of the cell are made of glass and the granular material used are 1.5 mm glass beads. The amplitude of vibration of the piezoelectrics is of the order of micrometres and the acceleration induced in the grains is about one tenth of the acceleration of gravity. The piezos are excited by a 400 Hz square signal with a maximum effective voltage $V_{\text{eff}} = 9$ V. The cell allows one to combine different measurements (see figure 8):

(i) an inductive probe provides the position of a thin metallic lid lying on the top of the granular surface and gives information about the mean compaction or potential energy of the packing,

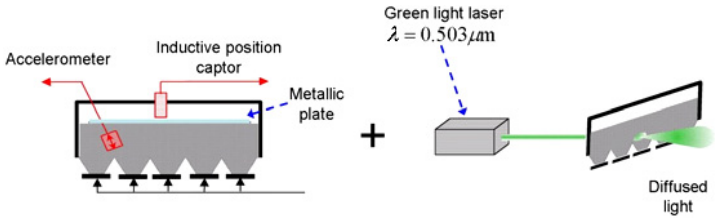

Figure 8. We can measure in the system the compaction, the effective injected power and the characteristic microscopic relaxation times (diffusing wave spectroscopy: DWS).

(ii) an accelerometer buried in the granular packing provides information on the effective injected power,

(iii) finally, a diffusing wave spectroscopy (DWS) is used to measure the characteristic times involved in the microscopic dynamics [19].

Preliminary results of experiments made in this set-up are reported in [20]. A slow logarithmic global compaction with diffusive-like fluctuations much smaller than the volume of a single grain was found, suggesting that there was no individual grain migration. DWS measurements revealed intermittent dynamics and it was possible to obtain a characteristic decorrelation time associated with each vibration intensity. It was pointed out in [20] that it would be interesting to couple all the different measures together to try to relate the microscopic features (characteristic correlation times and intermittent dynamics) to the macroscopic ones (compaction dynamics and density fluctuations) as well as to study their evolution in time and their behaviour in a stationary state. The experiments presented below are the first steps in this direction.

3.2. Compaction dynamics

The preparation procedure consisted in filling the container with the grains trying to make a free surface as horizontal as possible. Then, the lid was placed on the surface and some gentle taps were applied to compact the grains so as to 'erase' the structural memory of the pouring. Finally, the laser and the piezos were turned on. Long time experiments were performed (about four days of vibration) at different vibration intensities, $V_{\mathrm{eff}} = 5, 6$ and 7 V.[1] Surface position was continuously measured and acceleration and DWS measurements were made at several different moments throughout the duration of the experiment.

Figure 9 shows the data for three typical experiments at different vibration intensities. Note that after four days of vibration there are strong fluctuations and dilation periods though there is still an important increment in the compaction; a steady state was not reached in any experiment. We still do not know whether the fact of not reaching a stationary state even after such long times is due to the extremely weak vibration intensities and/or to a possible slow crystallization process resulting from monodispersity of the grains. For this reason we are at present doing similar experiments with a bidisperse mixture.

Even if, at long timescales, the packing fraction continues to increase, the compaction dynamics becomes very slow compared to the typical timescale of the fluctuations. Thus, for short times (of the order of one hour) we can talk of a quasi-stationary state.

[1] Which approximately correspond to accelerations in the bulk measured with the accelerometer of 0.65, 0.75 and 0.8 m s^{-2} respectively.

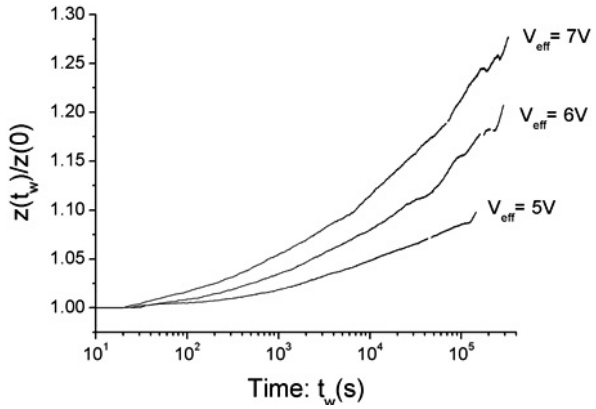

Figure 9. Typical compaction curves for three different vibration intensities: $V_{\rm eff} = 5, 6$ and 7 V. $z(t)$ is the sensor–lid separation (an increment in z corresponds to a higher compaction).

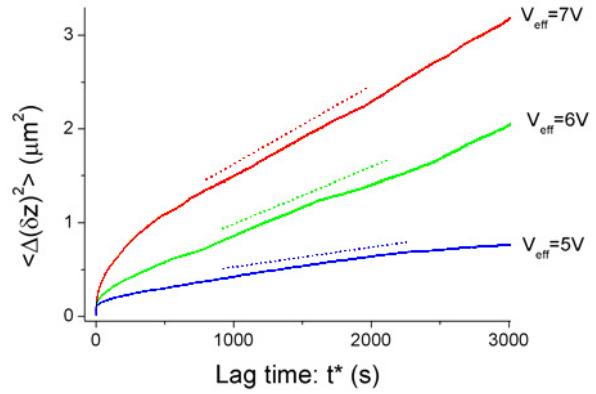

Figure 10. Function (3) for some of our data, averaged among experiments at equal $V_{\rm eff}$.

3.3. Free surface fluctuations

The energy fluctuations as a function of time have a central role in the context of the analogy between vibrated grains and thermal systems out of equilibrium [8, 9, 21]. The main idea is to adapt a fluctuation-dissipation relation to this kind of system. In our experiment the potential energy is proportional to the height of the free surface and its fluctuations are those of the surface position or, equivalently, of the lid–sensor separation $z(t)$:

$$\langle \Delta z^2(t) \rangle = \langle (z(t) - \langle z(t) \rangle)^2 \rangle. \tag{2}$$

Since we do not have enough experiments to do ensemble averages we have to replace the latter by a time average. To do such a time averaging for our quasi-stationary state we consider the time quantity $\delta z(t, t^*) \equiv z(t + t^*) - z(t)$ with average $\overline{\delta z(t^*)}$. Then, the fluctuations are

$$\overline{\Delta(\delta z(t^*))^2} = \overline{(\delta z(t, t^*) - \overline{\delta z(t^*)})^2}. \tag{3}$$

Figure 10 shows the results of equation (3) averaging over three or four experiments for each of the three different vibration intensities. It can be seen that at this timescale the variance or fluctuation of the surface position grows approximately linearly with time, which accounts for the diffusive dynamics characterized by an effective diffusion constant $\overline{\Delta(\delta z(t^*))^2} = D_{\rm eff} t^*$.

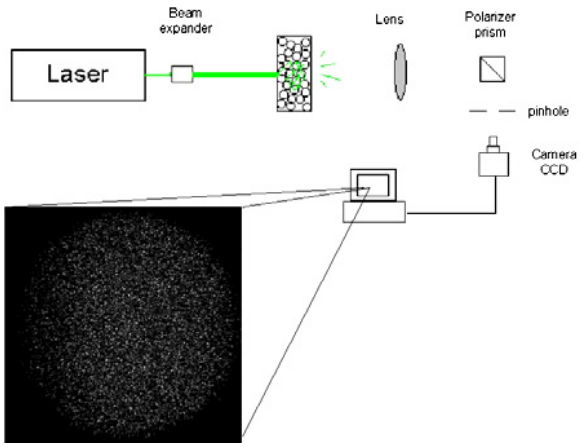

Figure 11. Experimental set-up used for the diffusion wave spectroscopy.

Note that this does not mean that there is individual particle diffusion; it has been checked that this is not the case. Instead, the diffusivity of the surface comes from a collective macroscopic behaviour.

3.4. DWS measurements

The basic idea of DWS is to make a coherent light (laser) pass through a scattering sample in which each photon is elastically scattered many times in such a way that it performs a random walk. Under these circumstances, the light diffuses through the sample and forms an interference pattern called speckle (see figure 11). The microscopic dynamics of the grains are related to the dynamics of the light interference pattern. The advantages of this technique are that it allows one to obtain information on the dynamics in the bulk of a 3D configuration and that it is sensitive to very small particle displacements (smaller than the wavelength of the light). Here, a multispeckle technique is used that was developed earlier for colloids [22–24]. The system dynamics is captured by computing the light intensity autocorrelation function:

$$g_2(t_w, t_w + t) \equiv \frac{\langle I(X, Y, t_w) I(X, Y, t_w + t)\rangle_{X,Y}}{\langle I(t_w)\rangle_{X,Y} \langle I(t_w + t)\rangle_{X,Y}} - 1 \tag{4}$$

where t_w is the time of the reference image with respect to the beginning of the experiment, t is the time relative to t_w and (X, Y) are the spatial coordinates on the speckle image. It is difficult to obtain a quantitative value for individual particle displacements from equation (4), especially in the case of glass beads, where particles are much bigger than the light wavelength and rotation plays a central role in the decorrelation of the interference pattern. However, characteristic relaxation times can be obtained precisely and allow one to access features of the dynamics like ageing and intermittency.

Figure 11 shows the scheme of the DWS set-up used in this experiment. This configuration is also used in [24].

In figure 12 a typical intensity autocorrelation function $g_2(t_x, t)$ (equation (4)) is shown. It was calculated 21 h after the beginning of the vibration for an experiment at $V_{\text{eff}} = 5$ V. This correlation function is well fitted by a stretched exponential [17]

$$y(t) = \exp(-(t/\tau)^{\alpha}). \tag{5}$$

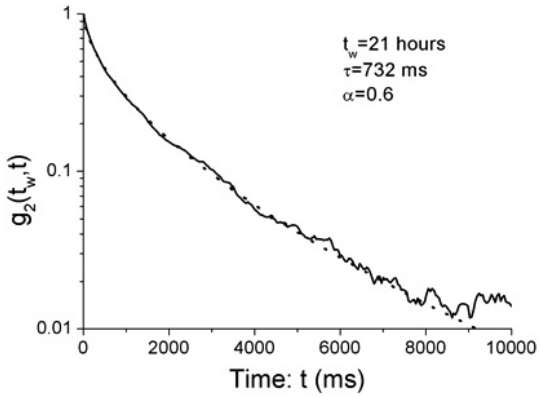

Figure 12. Typical correlation function (equation (4)) obtained from an experiment at $V_{\text{eff}} = 5$ V after 21 h of vibration. The dashed curve corresponds to a stretched exponential fit (equation (5)) from which we get a decorrelation time $\tau = 732$ ms and an exponent $\alpha = 0.6$.

From this fit we get two parameters that characterize the dynamics at a microscopic level: a decorrelation time τ and an exponent α. To determine the evolution over time of these parameters, measurements at smaller time intervals are necessary. We are actually working on these measurements which will give us the possibility of a very precise study of ageing of the system.

3.5. Relation between microscopic and macroscopic measures

In the context of the analogy between granular materials and thermal glassy systems [3, 5, 25] as well as in the application of statistical physics concepts to granular media [6], the relation between macroscopic features, such as packing fraction, and microscopic ones, like individual particle displacements, has a particular relevance. The experiment presented here allows one, in principle, to study such a relation since, on one hand, the packing fraction is given by the position of the free surface $z(t)$ and, on the other hand, we can estimate the order of magnitude of the mean displacement of the grains in our system from the DWS measures. For the particular geometry of our system it is a good approximation to consider that all the optical paths that constitute the interference pattern are equivalent random walks and have the same length [19]. It turns out that the number of steps of the random walk performed by the light through the grains is $n_{\text{s}} = (L/l^*)^2$, where L is the width of the system and l^* is the transport mean free path of the light. Then, the number of grains on one optical path is $n_{\text{g}} = n_{\text{s}}(l^*/d)$, where d is the diameter of the grains. On the other hand, the characteristic time τ of decorrelation of the intensity of light is given by the time during which an optical path changes by one wavelength λ. Considering again a random walk of the light, the average distance that a particle moves in time τ is $\epsilon \approx \lambda l^*/L$ [19]. We can estimate this distance for our experiment, where $L \approx 20$ mm, $d = 1.5$ mm and $\lambda = 512 \times 10^{-9}$ m. Besides this, experiments on the transmission of light by Pitois *et al* [26] suggest $l^* \approx d$ for our system[2]. Thus, we obtain for our system $\epsilon \approx 40$ nm. It is clear that the relaxation time τ characterizes the degree of agitation of the system at a microscopic level and that it is able to 'see' very small displacements of the grains. Now, we can try to understand the way in which this individual small displacements sum to give place to the macroscopic density fluctuations. To this end we plot D_{eff} as a function of τ from our

[2] In fact, this condition guaranties that we are indeed in the regime of diffusion of light.

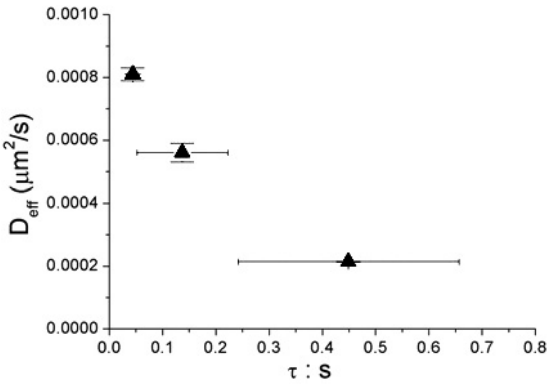

Figure 13. Effective diffusion constant of the free surface as a function of the inverse of τ, the characteristic correlation time obtained from DWS.

measurements in figure 13. The limited number of points at present prevents us from proving a clear relationship between these two quantities, but we have shown that this can eventually be established with our set-up. Once the relationship is established, we will be able to elaborate a model linking these two quantities.

3.6. Perspectives—2D model packing randomly shaken

In the previous section we presented the results obtained for a 3D granular assembly subjected to random agitation. In this case a random and spatially homogeneous agitation of the granular packing was achieved by using acoustic tweeters to inject sound at a very high frequency compared to the consequent motion of the grains. The technique allows us to work at accelerations much smaller than that due to gravity and thus in a regime where convection does not play a role. For this set-up we studied macroscopic properties like the fluctuations of the height of the assembly as well as microscopic quantities like the time for the displacement of a grain by of the order of 40 nm, using a DWS technique. However the access to local properties is, in 3D, always indirect. It is thus of interest to study in parallel a 2D set-up that allows direct access to the individual displacements of the grains. We use the following model system: a layer of polydisperse particles is confined between two vertical glass plates (20 cm $\times$ 30 cm). We use a mixture of small cylindrical particles with different diameters (4, 5, 6 mm) to create a disordered packing. First experiments using simple tapping showed however that convection (most likely induced by friction at the walls) is very important [20]. This convection can be suppressed by putting a lid on top of the cell, but then the position of the lid has to be finely tuned. A lid too close to the packing might suppress the granular motion drastically and a lid too far away from the packing might start convection again. Clearly this is not a method suited for studying a problem where compaction, i.e. the packing height, may vary.

We thus study a different system that allows for a much richer analysis. We have built a set-up where a large number of individually controlled pistons are moving up and down at the bottom of the cell described above. The individual control of these pistons allows one to go from spatially and temporally coherent to more complex and also completely random agitation. Furthermore, we can vary the frequency of the pistons over a quite broad range. Different accelerations going from below g to several g can also be applied. This set-up will, on the one hand, allow us to study the appearance and suppression of convection as a function

of the above-mentioned parameters; this will then allow us to study for example the compaction dynamics as a function of this phenomenon, a question that might lie at the origin of the different results obtained by Knight *et al* [16] and Bideau *et al* [14]. On the other hand, macroscopic parameters such as the fluctuations of the height of the assembly can then be studied over a wider range of parameters, as was possible for the 3D set-up (notably the crossover from low accelerations to accelerations higher than g) and might then be placed in relation with the results obtained there. And of course the transport and diffusion properties of a tracer particle could be determined directly and also be compared to the above-mentioned results.

4. Conclusion

In this paper we presented different experiments on dense granular materials close to the jamming transition. They differ in the way in which an external perturbation is applied to the system. In one case the system is initially at rest in a state of mechanical equilibrium under gravity (jammed state). The system is subjected to a local perturbation to unjam its structure. In the other case, vibration energy is applied at the bottom of the granular assembly in a novel way.

In the first case, we experimentally determine the reorganization field due to a small localized cyclic displacement applied to a packing of hard grains under gravity. The response to an upward perturbation can be separated into three distinct parts. Far from the intruder we observe a dominant radial displacement field whose amplitude scales as the inverse of the distance of the perturbation. Close to the perturbation we observe displacement rolls on both sides as well as a vault forming in the immediate surrounding of the intruder. In the part below the intruder, the displacement decays rapidly to zero. A local arching effect progressively screens the perturbation as seen far from the intruder and is accompanied by an irreversible displacement field. This irreversible field is too small to induce noticeable changes in the compactness but is sufficient to modify the subsequent mechanical response. Thus the granular material can be seen as an auto-adaptive material screening the exerted perturbation. Once this flow ceases the response is quasi-reversible but on each realization we still observe a remanent irreversible flow spanning the whole container and characterized by a different symmetry: vortex-like structures and coherent long range streams.

In the second case we report results obtained in a 3D granular assembly that is subject to an agitation produced by sound injection. This novel way of vibration allows fine tuning of the quasi-random input of energy into the system at accelerations much lower than gravity and could thus be considered as a kind of ‘thermal bath’. In this case we combine different measurements to characterize simultaneously microscopic and macroscopic properties of the system. In detail we measure the macroscopic compaction dynamics and density fluctuations by determining the position of the free surface of the system. We find a slow logarithmic global compaction with diffusive-like fluctuations much smaller than the volume of a single grain, suggesting that there is no individual grain migration and that the diffusion of the surface is thus likely to be due to collective macroscopic behaviour. From these measurements we extract an effective diffusive constant for the compaction fluctuations which is shown to increase with vibration intensity. Furthermore we use a DWS technique to access the characteristic timescales involved in the microscopic dynamics. We find intermittent dynamics and it was possible to obtain a characteristic decorrelation time associated with each vibration intensity. In addition we can estimate the average distance an individual particle can move in time. Our measurements allow us now to relate the macroscopic effective diffusion constant from the fluctuations of the free surface to the microscopic dynamics, given by a correlation time associated with an average particle displacement. We have reported preliminary results from

these measurements. More detailed experiments will in the future allow us to establish the exact relationship between these two quantities. This will give insight into the link between the individual particle displacement and the collective macroscopic behaviour of the system. The information obtained from these different experiments allows for a better understanding of the response of granular media close to the jamming transition which are subject to different external perturbations.

The third experimental set-up is only in its preliminary development stage. It consists of a 2D model packing of grains, similar to what is presented in the first part, but here the injection of energy is done by individual pistons placed at the bottom of the packing. The aim of the experiment is to be complementary to the sound injection method, as we can directly visualize the dynamical aspects of the flow and correlated motion between the grains.

Acknowledgments

We thank Philippe Claudin for fruitful discussions. This project is part of ECOS M03P01 and GC is supported by CONACYT and DGEP.

References

[1] Herrmann H J, Hovi J-P and Luding S (ed) 1998 *Physics of Dry Granular Media* (New York: Kluwer–Academic)
[2] Jaeger H M, Nagel S R and Behringer R P 1996 *Rev. Mod. Phys.* **68** 1259
[3] Ediger M D, Angell C A and Nagel S R 1996 *J. Phys. Chem.* **100** 13200
[4] Cates M E and Evans M R 2000 *Soft and Fragile Matter: Nonequilibrium Dynamics, Metastability and Flow* (Bristol: Institute of Physics Publishing)
[5] Liu A J and Nagel S R 1998 *Nature* **396** 21
[6] Edwards S F 1998 *Physica* A **249** 226–31
[7] Barrat A, Kurchan J, Loreto V and Sellitto M 2000 *Phys. Rev. Lett.* **85** 5034
Barrat A, Kurchan J, Loreto V and Sellitto M 2001 *Phys. Rev.* E **63** 051301
[8] Fierro A, Nicodemi M and Coniglio A 2002 *Phys. Rev.* E **66** 061301
[9] Crisanti A and Ritort F 2004 *Europhys. Lett.* **66** 253–9
[10] Kolb E, Cviklinski J, Lanuza J, Claudin P and Clément E 2004 *Phys. Rev.* E **69** 031306
[11] Reydellet G and Clément E 2001 *Phys. Rev. Lett.* **86** 3308
Serero D *et al* 2001 *Eur. Phys. J.* E **6** 169
Geng J *et al* 2001 *Phys. Rev. Lett.* **87** 035506
[12] Albert I *et al* 2001 *Phys. Rev.* E **64** 061303
[13] Philippe P and Bideau D 2002 *Europhys. Lett.* **60** 677
[14] Philippe P and Bideau D 2003 *Phys. Rev. Lett.* **91** 104302
[15] Nowak E R, Knight J B, Ben-Naim E, Jaeger H M and Nagel S 1998 *Phys. Rev.* E **57** 1971
Josserand C, Tkachenko A, Mueth D and Nagel S 2000 *Phys. Rev. Lett.* **85** 3632
[16] Knight J B, Fandrich C G, Lau C N, Jaeger H M and Nagel S R 1995 *Phys. Rev.* E **51** 3957
[17] Kabla A and Debrégeas G 2004 *Phys. Rev. Lett.* **92** 035501
[18] Pouliquen O, Belzons M and Nicolas M 2003 *Phys. Rev. Lett.* **91** 014301
[19] Weitz D A and Pine D J 1993 Diffusing-wave spectroscopy *Dynamic Light Scattering: The Method and Some Applications* (*Monographs on the Physics and Chemistry of Material* vol 49) ed W Brown (Oxford: Oxford University Press) pp 652–720
[20] Caballero G, Lindner A, Ovarlez G, Reydellet G, Lanuza J and Clément E 2004 *Unifying Concepts in Granular Media and Glasses* ed A Coniglio, A Fierro, H J Herrmann and M Nicodemi (Amsterdam: Elsevier B. V.) pp 78–92
[21] Makse H A and Kurchan J 2002 *Nature* **415** 614
[22] Wong A P Y and Wiltzius P 1993 *Rev. Sci. Instrum.* **64** 2547
[23] Cipelletti L and Weitz D A 1999 *Rev. Sci. Instrum.* **70** 3214
[24] Knaebel A, Bellour M, Munch J P, Viasnof V, Lequeux F and Harden J L 2000 *Europhys. Lett.* **52** 73
[25] Coniglio A and Herrmann H J 1996 *Physica* A **225** 1
[26] Pitois O, Höhler R and Cohen-Addad S 2000 *Proc. Colloque 'Physique et Mécanique Des matériaux Granulaires (Champs-sur-Marne (France))* p 199